

# Comparative Oncogenomics Implicates the Neurofibromin 1 Gene (*NF1*) as a Breast Cancer Driver

Marsha D. Wallace,<sup>\*,†</sup> Adam D. Pfefferle,<sup>\*,§,1</sup> Lishuang Shen,<sup>\*,1</sup> Adrian J. McNairn,<sup>\*</sup> Ethan G. Cerami,<sup>\*\*</sup> Barbara L. Fallon,<sup>\*</sup> Vera D. Rinaldi,<sup>\*</sup> Teresa L. Southard,<sup>\*,††</sup> Charles M. Perou,<sup>\*,§,††</sup> and John C. Schimenti<sup>\*,†,§§,2</sup>

<sup>\*</sup>Department of Biomedical Sciences, <sup>†</sup>Department of Molecular Biology and Genetics, <sup>††</sup>Section of Anatomic Pathology, and <sup>§§</sup>Center for Vertebrate Genomics, Cornell University, Ithaca, New York 14853, <sup>‡</sup>Department of Pathology and Laboratory Medicine, <sup>§</sup>Lineberger Comprehensive Cancer Center, and <sup>†††</sup>Department of Genetics, University of North Carolina, Chapel Hill, North Carolina 27514, and <sup>\*\*</sup>Memorial Sloan-Kettering Cancer Center, New York, New York 10065

**ABSTRACT** Identifying genomic alterations driving breast cancer is complicated by tumor diversity and genetic heterogeneity. Relevant mouse models are powerful for untangling this problem because such heterogeneity can be controlled. Inbred *Chaos3* mice exhibit high levels of genomic instability leading to mammary tumors that have tumor gene expression profiles closely resembling mature human mammary luminal cell signatures. We genomically characterized mammary adenocarcinomas from these mice to identify cancer-causing genomic events that overlap common alterations in human breast cancer. *Chaos3* tumors underwent recurrent copy number alterations (CNAs), particularly deletion of the RAS inhibitor *Neurofibromin 1* (*Nf1*) in nearly all cases. These overlap with human CNAs including *NF1*, which is deleted or mutated in 27.7% of all breast carcinomas. *Chaos3* mammary tumor cells exhibit RAS hyperactivation and increased sensitivity to RAS pathway inhibitors. These results indicate that spontaneous *NF1* loss can drive breast cancer. This should be informative for treatment of the significant fraction of patients whose tumors bear *NF1* mutations.

**T**WIN and family studies indicate that only ~25% of breast cancer cases have a heritable basis, and thus the majority (~75%) appear to be “sporadic” (Lichtenstein *et al.* 2000). Hence, much effort is now being placed on genomic analysis of breast and other cancers, focusing on cancer genome alterations in addition to inherited genetic variation. Comprehensive large-scale studies have been, and are being conducted in an attempt to identify genes and pathways that are commonly altered in various cancers, and which may thus represent cancer “drivers” with causative roles. However, the prevalence of passenger mutations, genetic heterogeneity, and the diversity of tumor etiologies and subtypes complicates unequivocal identification of drivers. Therefore, validation of cancer drivers—especially novel ones—requires orthogonal lines of evidence and exper-

imental confirmation. In this regard, mouse models can play an important role.

One putative cancer driver that has emerged is *NF1* (Neurofibromin 1). Best known for causing the autosomal dominant genetic disorder neurofibromatosis type 1, cancer genome resequencing studies are finding evidence that *NF1* is mutated (either by deletion or intragenic mutation) at significant rates in different cancers. *NF1* is a negative regulator of the RAS oncogene. It stimulates the GTPase activity of RAS (and thus is a “RasGAP”), pushing it to the inactive GDP-bound state. *NF1* is the third most prevalently mutated or deleted gene in glioblastoma multiforme (GBM) (The Cancer Genome Atlas Research Network 2008), one of the most significantly mutated genes in lung adenocarcinoma (Ding *et al.* 2008), and the fourth most (intragenically) mutated gene in ovarian carcinoma (The Cancer Genome Atlas Research Network 2011). Although *NF1* alteration has not yet been implicated as a significant breast cancer driver, loss of heterozygosity (LOH) of *NF1* has been noted in occasional cases (Guran and Safali 2005; Lee *et al.* 2010), as have intragenic mutations (Stephens *et al.* 2012). Women with neurofibromatosis type 1 (NF-1; a result of inheriting a mutant

Copyright © 2012 by the Genetics Society of America  
doi: 10.1534/genetics.112.142802

Manuscript received June 10, 2012; accepted for publication July 22, 2012

Supporting information is available online at <http://www.genetics.org/lookup/suppl/doi:10.1534/genetics.112.142802/-/DC1>.

<sup>1</sup>These authors contributed equally to this work.

<sup>2</sup>Corresponding author: College of Veterinary Medicine, Cornell University, Ithaca, NY 14850. E-mail: jcs92@cornell.edu.

*NF1* allele), have an increased risk of, or association with, breast cancer (Sharif *et al.* 2007; Salemis *et al.* 2010). Additionally, siRNA-mediated *NF1* knockdown in epithelial-like breast cancer cells induced the expression of epithelial-to-mesenchymal transition-related transcription factors (Arima *et al.* 2009). However, it remains uncertain whether the *NF1* mutations in these cases actually contribute to cancer etiology or maintenance.

Here, we took a comparative oncogenomic approach for breast cancer driver identification, exploiting the highly relevant mouse model C3H-*Mcm4*<sup>Chaos3/Chaos3</sup>. These mice bear a point mutation in the minichromosome maintenance 4 (*Mcm4*) gene that destabilizes the essential MCM2-7 replicative helicase. The resulting genomic instability (GIN) causes >80% of nulliparous females to develop mammary adenocarcinomas exclusively (Shima *et al.* 2007). The controlled genetic background and singular tumor etiology allows identification of recurrent mutational events likely to be involved in driving tumorigenesis. Strikingly, nearly all mammary tumors contained *Nf1* deletions. Furthermore, examination of The Cancer Genome Atlas (TCGA) data revealed that over a quarter of all human breast carcinomas are missing at least one copy of *NF1*. These findings indicate a potentially prominent role for spontaneous *NF1* aberrations in spontaneous breast cancers.

## Materials and Methods

### Mice

*Chaos3* mammary tumors originated in mice congenic in C3HeB/FeJ except 16898. *Chaos3* tumor 16898 and other *Chaos3* tumors arose in a mixed C57BL/6J and C3HeB/FeJ background. MMTV-neu and PyVT mammary tumors occurred in the FvB background.

### Microarray expression profiling

RNA was hybridized to custom murine Agilent microarrays and normalized as described (Herschkowitz *et al.* 2007, 2012). Data were deposited into the Gene Expression Omnibus (accession no. GSE36240). *Chaos3* tumors were clustered in relation to other mouse models using an unsupervised analysis, and differentiation score was calculated as described (Herschkowitz *et al.* 2007; Prat *et al.* 2010). Significance analysis of microarray (SAM) results were used to define a *Chaos3* gene signature (upregulated, FDR 0%), which was analyzed using the UNC337 human tumor data set (Prat *et al.* 2010). Genes significantly differentially expressed between *Chaos3* tumors and those of other mouse models are presented in [Supporting Information, File S1](#).

### Partial exome resequencing

A custom mouse 5-Mb Sequence Capture array (NimbleGen) was used to enrich DNA corresponding to ~1200 breast cancer candidate gene exons (File S2), followed by Illumina GAIIX sequencing. Candidate genes were selected and ranked

based on breast cancer specificity and frequency in primary literature, existing cancer arrays, and cancer databases.

The sequence capture was performed as follows. Genomic DNA libraries of ~200-bp fragment size were constructed for four *Chaos3* mammary tumors and one inbred C3H WT spleen following the standard protocol of Illumina (San Diego). One microgram of tumor and control library DNA was hybridized to the 385 K or 720 K capture array using an X1 mixer on the NimbleGen Hybridization system (Roche-NimbleGen) at 42° for 3 days. Arrays were washed; then the captured molecules were eluted from the slides using a NimbleGen Elution Station. Eluted molecules were vacuum dried and amplified by ligation-mediated (LM)-PCR. Real-time PCR of eight control amplicons was performed in the precapture and postcapture library to estimate the target fold enrichment, which varied from 30- to 744-fold.

The read data from each sample were aligned to the mouse C57BL/6, NCBI Build 37 (mm9) reference sequence using Novoalign (<http://novocraft.com>, v 2.05, academic version). Default alignment settings were used, but nonuniquely mapped reads or reads failing on alignment quality were discarded (-r NONE -Q 9). The percentage of on-target reads for mutant samples ranged from 34.5 to 62.9%, reflecting a 230-fold average enrichment for the target breast cancer candidate genes. Genome Analysis Toolkit (GATK) version 1.04413 was used sequentially for base quality recalibration, depth of coverage estimation, variant calling, and variant evaluation (DePristo *et al.* 2011). Substitution variants discovery and genotyping were performed with the GATK Unified Genotyper across all samples simultaneously. Single sample SNP calling was used to complement joint-sample SNP calling. The raw SNP calls were filtered per GATK recommendations with standard hard filtering parameters or variant quality score recalibration (DePristo *et al.* 2011). Criterion required SNP loci to have ≥5× coverage, variant frequency in ≥25% of reads, missing bases <30%, no significant strand bias, and not overlapping indels. Indels were called with GATK IndelGenotyperV2 under both single sample and paired sample modes using C3H as the “normal” tissue to identify novel indels against C3H. No novel indels were identified in targeted coding regions. Known SNPs between C3H and C57BL/6J were mined from the Mouse Genome Database (<http://www.informatics.jax.org/mgihome/projects/overview.shtml#snp>), dbSNP (Sherry *et al.* 2001), and Sanger Mouse Genome Project (Keane *et al.* 2011) (<http://www.sanger.ac.uk/resources/mouse/genomes/>). There were 3,097 known C3H SNPs in seqcap target regions from traditional Sanger sequencing. GATK joint estimation from in-house data identified 2990 filtered SNPs, representing a 96.6% sensitivity. Known C3H SNPs were filtered out, and novel SNPs were identified for annotation and validation. Variation consequence was annotated with Ensembl Variation API (<http://www.ensembl.org/info/docs/api/variation/index.html>) and custom perl scripts. Binary Sequence Alignment/Map (BAM), Blue Elephant Definition (BED), and Variant Call Format (VCF) files were generated to visualize alignments

and variations using the Integrative Genomics Viewer (IGV) software (Robinson *et al.* 2011). Variants were manually examined in IGV before proceeding to Sanger sequence validation as follows. Variant positions were amplified in corresponding tumor samples and inbred C3H control genomic DNA. Following Fast AP and Exo1 (Fermentas) treatment, PCR products were Sanger sequenced and analyzed using SeqMan. GeneCard, Ingenuity Pathway Tool, Biocarta, and KEGG databases were used to annotate genes.

### Array comparative genomic hybridization

Five micrograms of genomic DNA from tumor and reference samples were labeled and hybridized to  $3 \times 720$  K mouse Nimblegen CGH whole genome tiling arrays. The arrays consist of 50–75mer probes and a median spacing of 3.5 kb, with a subset of probes concentrated on exons. Two reference samples were used independently to ensure recurring CNAs were not artifacts caused by the reference sample. The first reference sample was collected from a C3H WT inbred mouse and run with tumor samples 2044b, 12351, and 12353. The second reference sample selected originated from a C3H congenic *Chaos3*<sup>+/+</sup> mouse and run as the reference for the remaining samples. DNA labeling, hybridization, and posthybridization processing were performed according to the manufacturer's protocol. Nimblegen software was used to normalize test/reference ratios and perform background correction. Copy number changes were identified and segmented with Nimblegen CGH-segMNT algorithm using un-averaged and 10× averaging windows. The significance threshold was set at  $\pm 0.15 \log_2$  ratio and required a minimum of two consecutive probes to exhibit a change in order to call a segment. Amplifications and deletions were visualized using Nimblegen software and confirmed by manually examining  $\log_2$  ratios for regions of interest. In addition to using Nimblegen software, the normalized  $\log_2$  ratio data were also analyzed using KCSmart software (Klijn *et al.* 2008) to identify significantly recurrent CNAs. The kernel width was 1 Mb, and the resolution of the sample point matrix was 5 Kb. Simple Bonferroni multiple testing correction  $P \leq 0.025$  was used as threshold for declaring significant regions. Select genes within CNAs were validated via qPCR. See File S3 for the primer list.

Human breast cancer data and CNA calls for comparison with *Chaos3* CNAs were taken from the publicly available Cancer Genome Atlas portal (<https://tcga-data.nci.nih.gov/tcga/tcgaHome2.jsp>) 2010 update. The regions considered to have undergone segmental deletions by the publicly available Cancer Genome Atlas analysis ("level 4" data set) are those indicated in Figure 2B. The Memorial Sloan-Kettering Cancer Center cBio portal provides a breakdown by mammary tumor subtype for individual genes (<http://www.cbioportal.org/public-portal/index.do>). According to the cBioPortal data available as of May 2012, the genes between the *NOS2* and *NF1* interval (which were not classified as significantly segmentally deleted in the limited level 4 data set mentioned above), are hemizygotously deleted at rates similar to

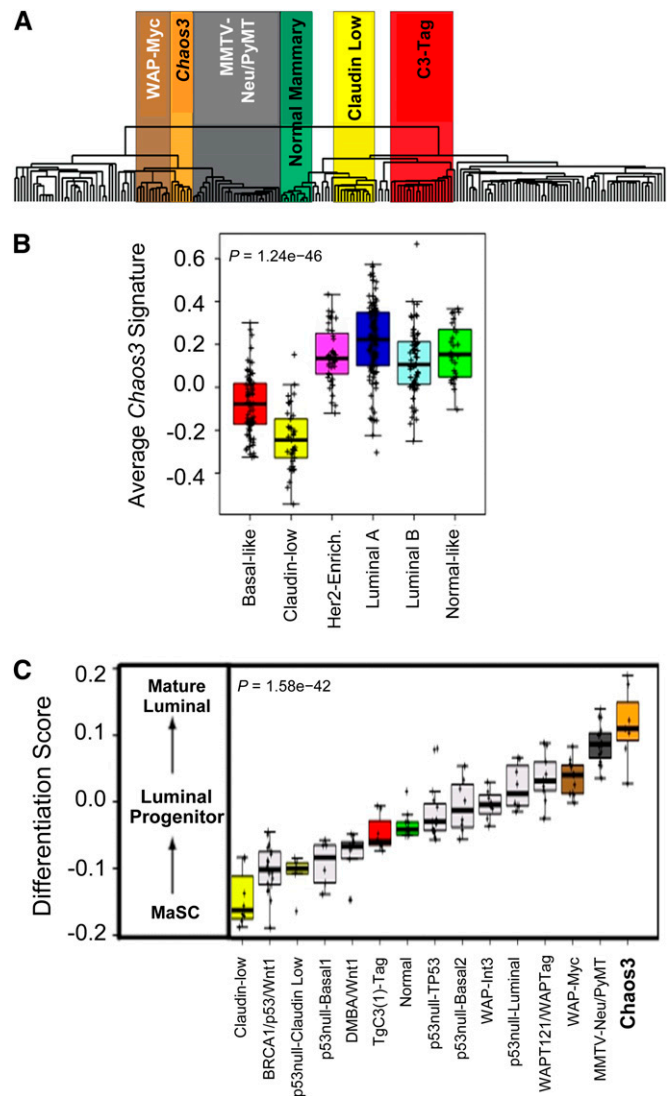


**Figure 1** *Chaos3* tumors model key human features. (A) Expression microarray dendrogram of *Chaos3* mammary tumors and 185 other mouse mammary carcinomas and normal mammary tissue samples. The *Chaos3* tumors cluster together as a distinct group near luminal murine models: MYC, PyMT, and Her2/Neu. Genes significantly differentially expressed between *Chaos3* tumors and those of other mouse models are presented in File S1. (B) Boxplot of the *Chaos3* gene signature in the UNC337 human breast tumor data set. *Chaos3* tumors have higher signature expression in human luminal, HER2-enriched, and normal-like intrinsic subtypes. (C) *Chaos3* differentiation score (*D* score) in relationship with other genetically engineered mouse models (GEMMs). The high *D* score shows that *Chaos3* tumors more closely resemble the expression signature of mature human luminal cells relative to all other mouse models analyzed. (B and C) *P*-values reflect statistical significance of ANOVAs. MaSC, mammary stem cell.

*NF1* itself. Critical regions within each *Chaos3* CNA were identified as the region with the greatest overlap across multiple *Chaos3* tumors.

### Cell culture experiments

Primary *Chaos3* tumor biopsies were homogenized, cultured, treated with colcemid, and metaphase spreads were made (Shima *et al.* 2007). Imaged chromosomes were counted

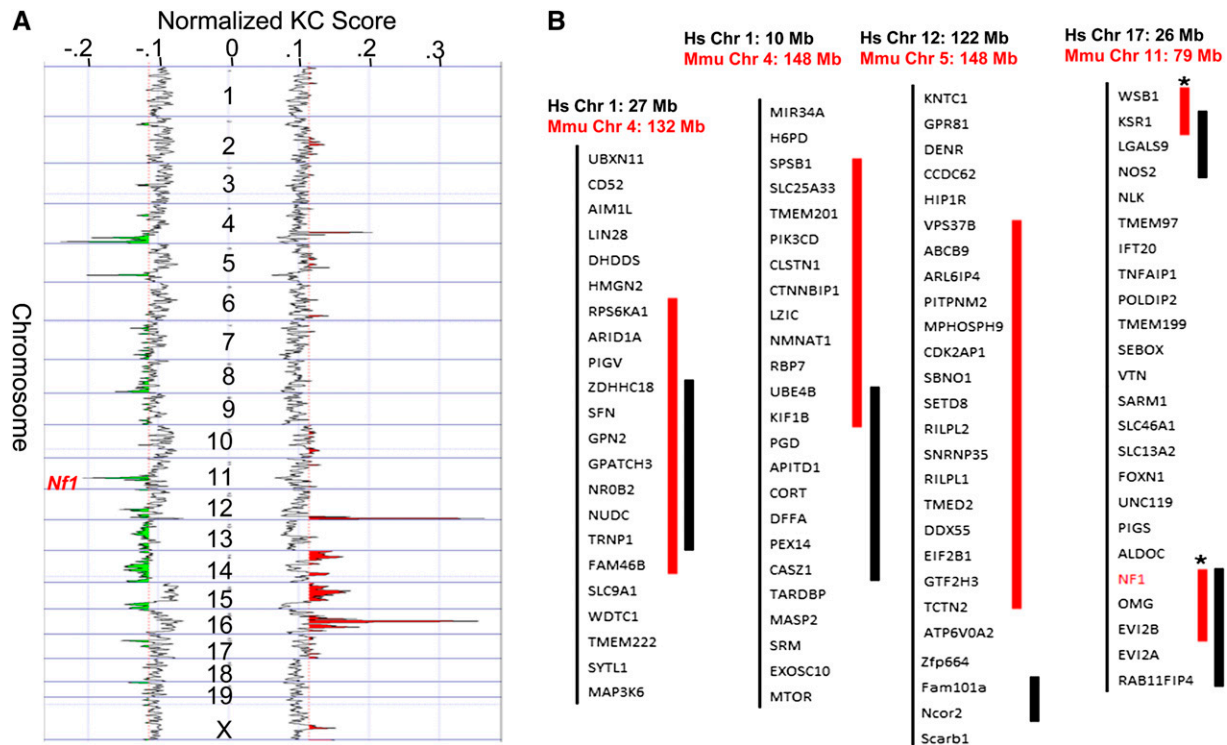


**Figure 2** Recurrent CNAs in *Chaos3* mammary tumors overlap with those in human breast cancer, including *Nf1* deletion. (A) KCSmart analysis of combined aCGH data from 12 *Chaos3* tumors, (nine mammary and three nonmammary). The most significant amplification peaks (red) lie on Chrs 12 and 16, and deletions (green) on Chrs 4, 5, and 11. (B) Overlap of mouse (Mmu) *Chaos3* recurrent deletions with human (Hs) breast tumor CNAs. Human gene orders are shown. Thick red bars indicate the critical regions of mouse deletions, the subregions that, among all alterations in those regions, are common across all or most *Chaos3* tumors. Of *Chaos3* tumors with CNAs in these regions, the percentage of those containing the critical region is as follows: Chr 4 132 Mb = 86%; Chr 4 148 Mb = 71%; Chr 5 = 86%; Chr 11 = 86% (100% for *Nf1*, *Ksr1*, and *Wsb1*). The thick black bars to the right of the gene symbols indicate corresponding recurrent segmental CNAs in human breast cancers (limited level 4 data set from TCGA). Note that the Chr 11 deletions are single events in mice (asterisks on red part indicate these sequences are juxtaposed and contiguous in the mouse genome), and it is possible that the interval between *NOS2* and *NF1* may also be deleted as single events in human breast cancers, since the intervening genes are present in the hemizygous state in a high percentage of tumors according to extended TCGA data sets.

using ImageJ. Tumor cell lines were treated with the MEK1 inhibitor PD98059 or MTOR inhibitor rapamycin (Chang *et al.* 2007; Leong *et al.* 2010). Cell proliferation was assessed via 3-(4,5-Dimethylthiazol-2-yl)-2,5-diphenyltetrazolium bromide (MTT) assay (Sigma) and values read on a 96-well ELISA plate reader.

#### Active RAS pull-down and Western blotting

Levels of activated RAS were obtained using an active RAS pull-down kit (Thermo Scientific). Rabbit anti-NF1 (Novus Biologicals) was used at 2  $\mu$ g/ml for Western analyses.

## Results

### Gene expression profiling reveals that the *Mcm4<sup>Chaos3/Chaos3</sup>* mouse is a highly relevant luminal breast cancer model

Human breast tumors can be classified into subtypes using gene expression signatures that are also conserved within mouse models of mammary cancers (Perou *et al.* 2000; Herschkowitz *et al.* 2007). *Mcm4<sup>Chaos3/Chaos3</sup>* mammary tumors (referred to as “*Chaos3*”) are histologically classified as adenocarcinomas (Shima *et al.* 2007), and comparison with

the 185 mouse mammary tumor data set of Herschkowitz *et al.* (2012) shows clustering near three luminal adenocarcinoma mouse models (Figure 1A). Consistent with this, the *Chaos3* gene signature was most highly expressed in the human luminal A subtype, and was also high in HER2-enriched and luminal B tumors (Figure 1B). Luminal breast tumors are the most prevalent type in humans (Carey *et al.* 2006). SAM revealed that *Chaos3* tumors have a distinct gene expression pattern from all other mouse models, including dramatic upregulation of *Muc11*, a diagnostic marker in human breast cancer (Table S1) (Hube *et al.* 2004). Tumor differentiation score (*D* score) analysis showed that *Chaos3* tumors more closely resemble mature human luminal cells than any mouse model analyzed to date (Figure 1C). Together, these results show that *Chaos3* mice are an excellent human breast cancer model.

### Evidence that *Chaos3* mammary tumors are driven by recurrent CNAs overlapping those common to human breast cancers

Primary *Chaos3* cells have increased stalled replication forks that persist through metaphase, leading to chromosome breaks and improper chromosomal segregation (Shima *et al.*

**Table 1 Recurrent copy number alterations in Chaos3 tumors**

Tumor/sample type	Sample name	Boundaries (Mb)								
<b>Amplifications</b>										
Chaos3 MT	15259	Chr 16 45–54	Chr 16 38–39	Chr 12 114–117	Chr 17 13–14	Chr 17 77–78	Chr 16 27M	—	—	—
Chaos3 MT	12351L	45.8	38.8	114.5	13.4	—	—	—	—	—
Chaos3 MT	12351L	50.4	39.6	117.1	13.7	—	—	—	—	—
Chaos3 MT	12353A	45.8	38.8	114.7	—	—	—	—	—	—
Chaos3 MT	12115B	50.5	39.0	117.1	—	—	—	—	—	—
Chaos3 MT	12115B	44.9	38.8	qPCR	—	—	—	—	—	—
Chaos3 MT	12352	45.1	38.8	114.7	—	77.5	27.6	27.7	—	—
Chaos3 MT CL	2044B	45.8	38.8	114.6	13.3	—	—	—	—	—
Chaos3 MT	11929A	45.8	38.8	117.1	13.2	—	—	—	—	—
Chaos3 MT	16168	47.3	—	114.7	—	78.1	27.6	27.7	—	—
Chaos3 MT	16898	46.3	—	114.7	13.2	76.3	—	—	—	—
Chaos3 Mdl	17883	45.1	38.8	114.7	13.3	77.2	27.6	27.7	—	—
Chaos3 HS Uterus	16862	45.8	38.8	114.7	—	—	27.6	28.0	—	—
Chaos3 BT	10658	45.8	38.8	114.7	—	—	27.6	27.7	—	—
MMTV-Neu MT	3750	45.8	—	115.2	3.5	67.2	—	—	—	—
MMTV-Neu MT	3744	46.3	38.8	117.2	—	76.4	—	—	—	—
Deletions										
Chaos3 MT	15259	Chr 11 78–79	Chr 5 124–125	Chr 4 148–149	Chr 4 132–133	Chr 10 79–80	Chr 19 3–7	Chr 19 32–33	—	—
Chaos3 MT	12351L	78.9	124.3	148.6	132.7	79.9	4.0	—	—	—
Chaos3 MT	12353A	78.5	—	149.1	—	—	3.9	—	—	—
Chaos3 MT	12115B	78.1	123.5	147.6	133.0	78.1	—	—	—	—
Chaos3 MT	12115B	79.6	125.1	150.1	132.9	—	—	—	—	—
Chaos3 MT	12352	78.9	122.7	148.6	131.9	—	—	—	—	—
Chaos3 MT CL	2044B	qPCR	124.5	148.1	131.9	80.6	—	—	—	—
Chaos3 MT	11929A	78.6	123.8	149.1	133.0	79.8	4.2	4.8	33.1	33.5
Chaos3 MT	16168	78.9	124.3	qPCR	133.2	79.0	—	—	—	—
Chaos3 MT	16898	qPCR	—	148.1	—	—	—	—	—	—
Chaos3 F1 MT	17883	78.2	124.9	148.4	132.6	79.0	3.0	7.5	—	—
Chaos3 HS Uterus	16862	—	—	—	—	—	—	—	—	—
Chaos3 BT	10658	—	—	—	131.2	79.4	—	—	—	—
MMTV-Neu MT	3750	—	—	147.2	131.3	—	—	—	—	—
MMTV-Neu MT	3744	—	—	155.6	122.2	79.0	3.0	9.2	26.0	61.3
MMTV-Neu MT	3744	—	—	122.2	155.6	79.0	—	—	—	—

Recurring CNAs among 12 Chaos3 tumors and two MMTV-Neu mammary tumors identified by aCGH. The values are physical locations of the deleted or amplified regions according to the mouse genome sequence. In some cases, map locations were refined by qPCR as indicated. Samples analyzed are primary tumors except where indicated. MT, mammary tumor; CL, cell line; HS, histiocytic sarcoma; Mdl, mediastinal tumor; BT, bone tumor.

**Table 2 Cancer and immunity-related genes in *Chaos3* mammary tumor CNAs**

Function	Amplified		Function	Deleted				
	Chr 16	Chr 12		Chr 4	Chr 5	Chr 11	Chr 10	Chr 19
Pluripotency	<u><i>Dppa4, Dppa2</i></u>		Tumor suppressor		<u><i>Cdk2ap1</i></u>	<u><i>Nf1*</i></u>		
Signal transduction		<i>Adam6*</i>	DNA checkpoint/repair		<u><i>Kntc1, Gtf2h3, Setd8</i></u>			<i>Rad9</i>
Immunity/inflammation	<u><i>Pvr13, Retnlb, Retnla</i></u>	<i>Ig/abparts*</i>	Apoptosis/necrosis	<u><i>Dffa, Ube4b*</i></u>			<i>Oaz1*</i>	
Upregulated in cancer	<u><i>Igsf11</i></u>		Signal transduction	<u><i>Pik3cd</i></u>		<u><i>Ksr1*</i></u>	<i>Csnk1g2*</i> <i>Mknk2*</i> <i>Lingo3*</i>	
			Immunity/inflammation Cancer related	<u><i>Arid1a, Sfn*</i></u>	<u><i>Sbno1</i></u>			<i>Minpp1*</i>

The genes commonly altered specifically in mammary tumors are underlined, and those that additionally have CNAs in human breast cancers are marked with an asterisk. *Ig/abparts*, *Ig* locus and antibody parts gene feature conserved between mice and humans.

2007; Kawabata *et al.* 2011a,b). Similar to human breast tumors (Hanahan and Weinberg 2011), *Chaos3* tumors had high levels of aneuploidy and drastic variation in chromosome number, even within the cells of a single tumor (Figure S1). With such intratumor variation, we expect that only early and/or highly selected mutations would be readily detectable and highly recurrent across multiple cases. To uncover mutations potentially driving carcinogenesis in *Chaos3* mice, we first performed partial exome resequencing of mammary tumors. Surprisingly, we discovered few somatic point mutations in the targeted exonic regions and calculated the mutation rate at  $1.1 \times 10^{-7}$ , or 0.25 mutations/Mb, which is not above the background rate in other genomic studies of breast cancer (Greenman *et al.* 2007; Kan *et al.* 2010). The mutated genes are involved in diverse functions or are simply large (*i.e.*, Titin), and together they do not implicate a commonly affected pathway underlying carcinogenesis (Table S1). These results indicate that elevated intragenic mutagenesis is not the primary mechanism driving *Chaos3* carcinogenesis, and that other initiators such as CNAs may be responsible.

*Saccharomyces cerevisiae* containing the *Chaos3* mutation have elevated translocations as well as segmental amplifications and deletions (Li *et al.* 2009). To examine genomic copy number changes, we performed array comparative genomic hybridization (aCGH) on 12 *Chaos3* tumors (nine *Chaos3* mammary and three nonmammary), and two MMTV-*Neu* mammary tumors. *Chaos3* nonmammary tumors can be obtained by genetic perturbations or altering the strain background (Chuang *et al.* 2010; Kawabata *et al.* 2011b). Strikingly, the *Chaos3* tumors exhibited highly recurrent CNAs in a small number of regions. Nearly all tumors had amplifications on chromosomes (Chr) 12 and 16 regardless of tumor type (Figure 2A; Table 1). Deletions on Chrs 5 and 11 were found in *Chaos3* mammary tumors specifically, and there was a small commonly deleted region on Chr 4 that was shared by *Chaos3* and MMTV-*neu* mammary tumors (Table 1). We screened TCGA human breast cancer genomic data and found commonly deleted regions overlapping the syntenic regions of recurrent *Chaos3* deletions (Figure 2B, Table S2, and Table S3). Interestingly, the Chr 12 amplifications had

precise breakpoints (Table 1) that flank a region enriched in immunoglobulin (*Ig*) gene fragments. While none of the six recurrently amplified regions were unique to *Chaos3* mammary tumors, genes in these regions have roles in metastasis, pluripotency, signal transduction, or are upregulated in cancer (Table 2). The recurrently deleted regions contain several genes that overlap with human breast cancer CNAs and/or have potential or suggested roles in cancer: *Ube4b* (an ubiquitin ligase that negatively regulates *Trp53*) (Wu *et al.* 2011), *Kif1b* (a potential haploinsufficient tumor suppressor) (Munirajan *et al.* 2008), and *Rad9* (deleted in three of the nine tumors, it is involved in the Ataxia telangiectasia and Rad3 related (ATR) DNA damage response pathway; mutation or misregulation of this gene is associated with various cancers, including breast) (Lieberman *et al.* 2011) (Table 2, Table S2, and Table S3).

#### ***Nf1* is deleted in nearly all *Chaos3* mammary tumors and a high proportion of human breast cancers**

Particularly striking to us is the set of *Chaos3* deletions on Chr 11 that overlaps with a recurring cluster of CNAs on human Chr 17. All *Chaos3* mammary tumors examined by aCGH but none of the MMTV-*Neu* driven mammary tumors or *Chaos3* nonmammary tumors contained Chr 11 deletions (Figure 3, A and B, Table 1, Table S2, and Table S3). The small deletions have nested breakpoints that define a commonly deleted region, and all of which contained the tumor suppressor *Nf1* (Neurofibromin 1), *Omg* (oligodendrocyte myelin glycoprotein; this gene lies within an intron of *Nf1*), *Wsb1* (WD repeat and SOCS box-containing protein 1), and *Ksr1* (kinase suppressor of RAS) (Figure 3B). Except for *Nf1*, none have a plausible role as a mammary tumor suppressor. *Omg* is expressed primarily in neural tissues and is required for myelination in the central nervous system. *Ksr1* promotes oncogenic RAS and MAPK signaling in mice and cells, so its deletion would be expected to actually inhibit tumor growth (Lozano *et al.* 2003; Goettel *et al.* 2011). *WSB1* appears to participate in an E3 ubiquitin ligase complex not known to be associated with cancers. The gene *Rab11fip4*, which is deleted in many but not all of the *Chaos3* mammary tumors, acts as a regulator of endocytic traffic but

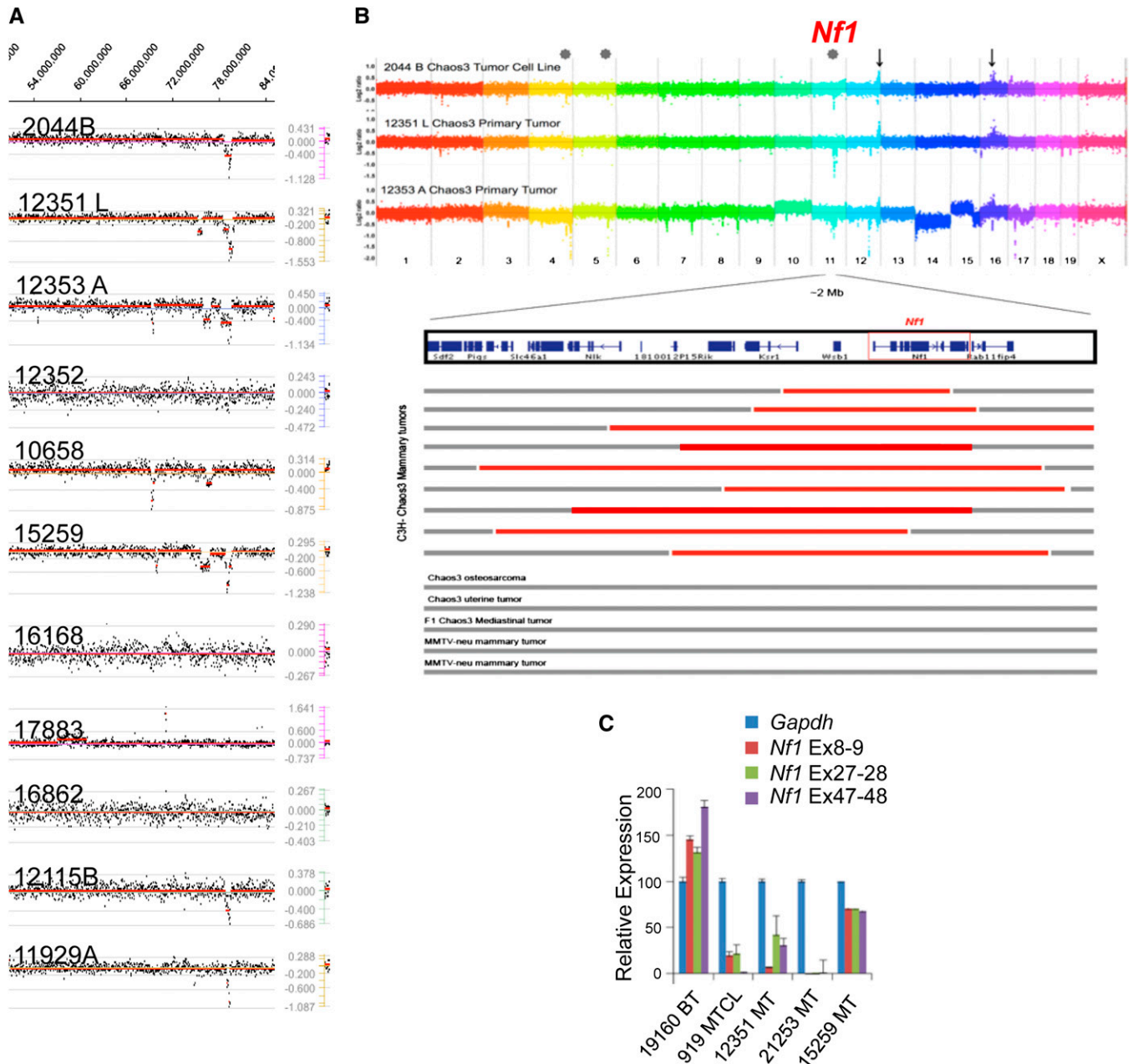


**Figure 3** *Nf1* is deleted in *Chaos3* mammary tumors. (A) Recurrent deletions detected by aCGH on Chr 11 at ~79 Mb, specific to *Chaos3* mammary tumors. The broken red line indicates significant log<sub>2</sub> ratios. Tumor 17883 is a mediastinal lymphoma/leukemic tumor, 16862 is a histiocytic sarcoma in the uterus, 10658 is a bone tumor, and the other tumors are mammary. Mammary tumors 16168 and 12352 did not have significant detectable deletion by aCGH, but did by qPCR (Table S4). (B, Top) aCGH results of two primary *Chaos3* mammary tumors and one *Chaos3* mammary tumor cell line. Dots substantially above the log<sub>2</sub> ratio line correspond to loci amplified in the tumor, and dots below are underrepresented. Arrows mark loci commonly amplified in *Chaos3* tumors regardless of tumor type, and asterisks mark commonly deleted loci segregating specifically with mammary tumors. (Bottom) Expanded view of Chr 11 deletion. Red bars indicate aCGH or qPCR confirmed deletion in all nine *Chaos3* mammary tumors overlapping *Nf1*. (C) qRT-PCR analysis of *Nf1* mRNA levels across the transcript in *Chaos3* tumors. Percentage of expression is relative to an MMTV-PyVT tumor as control, which does not have loss of *Nf1*. Error bars show standard error of the mean. Mammary tumor 15259 is heterozygously deleted for *Nf1*, and the others are homozygously deleted. Residual signal may reflect biopsy contamination or tumor heterogeneity.

is expressed predominantly in retina and neural tissues, with little or no detectable expression in mouse or human mammary tissue (microarray data viewable at BioGPS.org and GeneCards.org).  
 These data and information led us further to explore the potential role of *Nf1* as a driver of *Chaos3* mammary tumors.

We analyzed the DNA of the aCGH samples and additional *Chaos3* mammary tumors by qPCR. Overall, 59/60 contained *Nf1* deletions, with 51.6% appearing homozygous and 46.6% heterozygous (Table 3 and Table S4). *Nf1*-deleted tumors showed absence or severe reduction of mRNA and protein (Figures 3C and 4A). NF1 negatively regulates RAS, which

**Table 3 qPCR analysis of deletions in *Chaos3* mammary tumors**

		DNAs									
		15259	12351L	12353A	12352	2044B	11929A	16168	16898	12115B	WT
Chr 4	<i>Kif1b</i>	<b>53.0</b>	141.1	<b>77.8</b>	<b>25.9</b>	<b>61.3</b>		96.5			
	<i>Pik3cd</i>	<b>55.8</b>	134.6	89.9	<b>29.2</b>	<b>55.4</b>		103.3			
	<i>Eno1</i>	<b>58.7</b>	87.3	105.3	<b>39.3</b>	<b>51.5</b>		108.4			
	<i>Rere</i>	<b>51.7</b>	108.9	104.4	<b>32.4</b>	<b>48.9</b>		100.6			
Chr 11	<i>Slc46a1</i>	82.2							<b>36.7</b>		
	<i>Tnfaip1</i>	92.9	<b>71.4</b>	<b>79.3</b>		<b>65.0</b>	83.4	<b>59.8</b>			
	<i>Nlk</i>	103.6	<b>63.5</b>	105.4		<b>67.5</b>	116.0	<b>50.5</b>			
	<i>Nf1 (5')</i>	<b>17.4</b>	<b>35.5</b>	<b>25.5</b>	<b>12.7</b>	<b>63.7</b>	<b>16.7</b>	<b>9.2</b>		<b>31.2</b>	107.3
	<i>Omg (Nf1 3')</i>	<b>52.9</b>	<b>12.0</b>	<b>16.7</b>	<b>0.7</b>	<b>48.0</b>	<b>16.3</b>		<b>75.1</b>	<b>38.7</b>	109.4
	<i>Rab11fp4</i>	<b>49.8</b>							<b>65.9</b>		

qPCR values are presented in percentage of genomic DNA compared to C3H wild type. Boldfaced data indicate heterozygous or homozygous deletion (<80% control signal). Cancer-related genes, deleted at high frequency in mammary tumors specifically, are underlined. *Nf1* deletion was validated at the 5' and 3' ends of the gene (*Omg* lies within an intron near the 3' end of *Nf1*). Note that copy number differences between *Nf1* 5' and 3' are observed in some tumors, indicating a breakpoint within the *Nf1* gene. Deletion calls were made as follows: Heterozygous = 15–80%; homozygous = <15%; if either *Nf1* or *Omg* were <15%, the tumor sample was called as homozygously deleted (see text for overall summary; data for tumors not examined by aCGH are not shown here) because full *Nf1* transcripts cannot be made. Nucleotide positions are from the mm9 mouse assembly. Sample 2044B is a tumor-derived cell line. WT, wild type.

controls proliferation, differentiation, cell adhesion, apoptosis, and cell migration through the MAPK and PI3K signal transduction pathways (Figure 4B). RAS proteins are often deregulated in cancers, leading to increased invasion and metastasis and decreased apoptosis (Pylayeva-Gupta *et al.* 2011).

Best known for causing neurofibromas in the autosomal dominant genetic disorder neurofibromatosis type 1, women with inherited *NF1* deficiency also have an increased risk of, or association with, breast cancer (Sharif *et al.* 2007; Salemis *et al.* 2010). Though there are few reports implicating spontaneous *Nf1* loss in breast tumorigenesis (Guran and Safali 2005; Lee *et al.* 2010), upon screening TCGA breast cancer data sets we found that 27.7% of human breast tumors have *NF1* deletions or mutations, most being heterozygous (Figure 5A and File S4). Furthermore, >40% of basal and HER2-enriched tumor subtypes have *NF1* loss or mutations (Figure 5A). Genomic *NF1* deficiency in human breast tumors significantly correlated with decreased expression levels ( $P = 3.32 \times 10^{-13}$ ) (Figure 5B), both supporting the deletion calls and that the deletions impact *NF1* levels.

#### ***Chaos3* mammary tumors have hyperactivated RAS**

*NF1* is a negative regulator of the RAS signaling pathway that stimulates the GTPase activity of RAS, pushing it to the inactive state. *NF1* is important for negatively regulating the progrowth factor mTOR, which is stimulated by RAS (Figure 4B). Tumor cells of patients with acute myelogenous leukemia (AML) having *NF1* deficiency demonstrate an elevated level of activated RAS and sensitivity to the mTOR inhibitor rapamycin (Parkin *et al.* 2010). To assess the functional impact of *Nf1* deletion, we examined the level of activated RAS and found it to be dramatically higher in *Chaos3* mammary tumor cells deleted for *Nf1* (Figure 4A). We hypothesized that if the elevation of RAS signaling in *Nf1*-deleted mammary tumor cells is important for their maintenance, then inhibition of downstream pathways would compromise the growth of these cells. *Chaos3* mammary

tumor cell lines were markedly sensitive to MAPK/MEK1 and/or mTOR inhibitors, PD98059 and rapamycin, respectively (Figure 4C).

#### **Discussion**

Cancer genome resequencing studies are finding evidence that *NF1* is mutated (either by deletion or intragenic mutation) at significant rates in different cancers. The two major studies published by TCGA Research Network on glioblastoma multiforme and ovarian carcinoma both found that *NF1* and the PI3K/RAS pathway were mutated at significantly elevated rates (The Cancer Genome Atlas Research Network 2008, 2011). Though the TCGA Research Network has yet to publish its breast cancer genome data, the correlation between lower *NF1* expression and copy number (as called by their implementation of the GISTIC algorithm) supports their calls of *NF1* heterozygosity in the tumors they examined. Canonically, tumor suppressors are thought to require loss of both copies to have functional impact. However, there is accumulating evidence that haploinsufficiency or reduced expression of tumor suppressor genes can influence carcinogenesis (Berger *et al.* 2011). Indeed heterozygosity for *Nf1* causes cancer-like cellular phenotypes in astrocytes (Gutmann *et al.* 1999; Bajenaru *et al.* 2001; Gutmann *et al.* 2001). We note that a recent cancer genome study did not report a high frequency of *NF1* CNAs (Curtis *et al.* 2012). It is likely that the differences are related to different analytical methods of CNA calling and they highlight the need for follow-up analyses such as the qPCR we performed on the mouse tumors.

The mechanistic basis behind frequent deletion of *NF1/Nf1* as opposed to intragenic mutation is an intriguing question that could yield insight into etiology of cancers with *NF1* deletion. A combination of factors may contribute to *NF1* CNAs, including fragile sites in the vicinity (Figure S2), a complex chromatin structure, and/or the gene's large size. Replication fork stalling near *Nf1* has been noted at a 5-kb

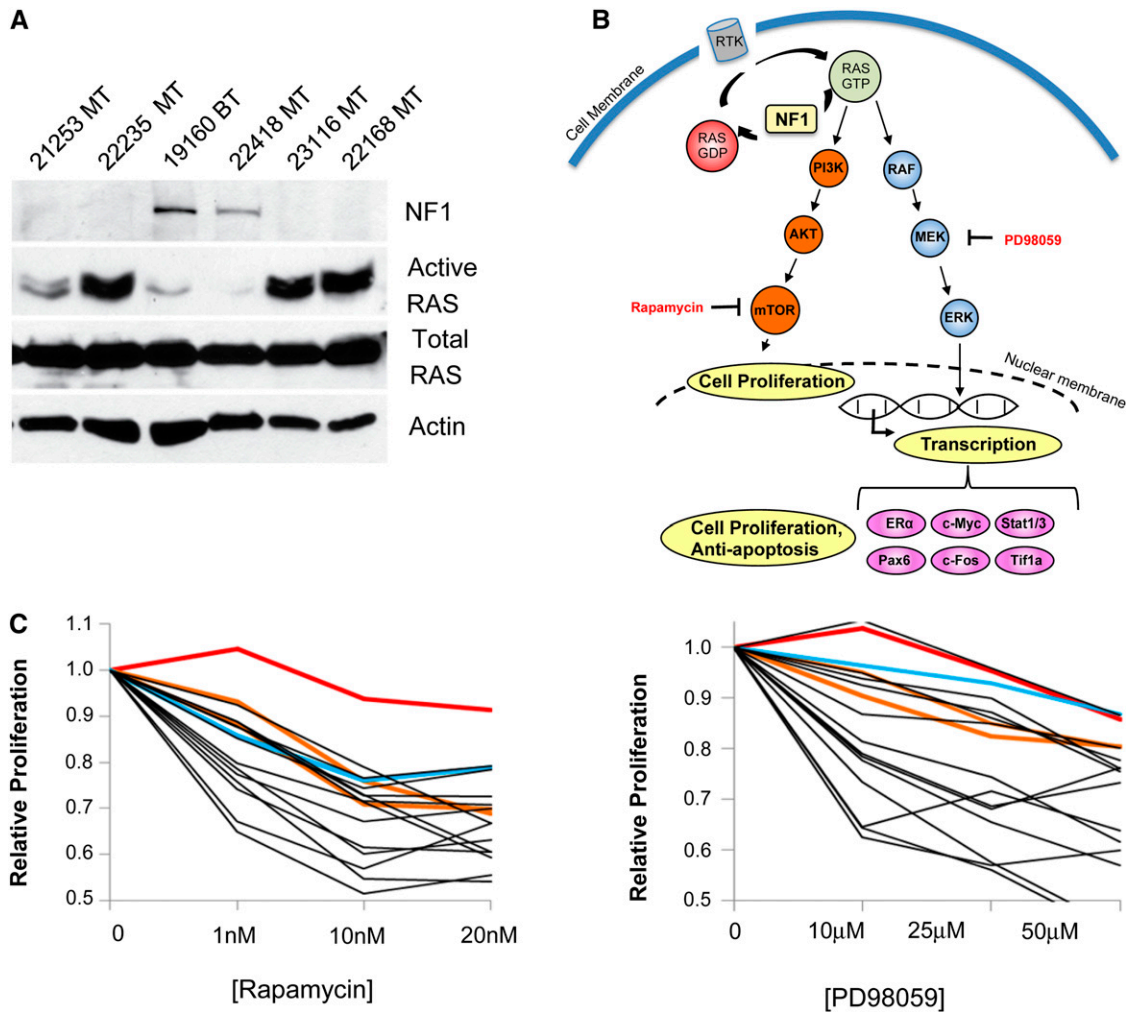


**Figure 4** *Nf1* deletion in *Chaos3* mammary tumors leads to increased activated RAS and sensitivity to PI3K and MAPK inhibitors. (A) Western blot analysis of *Chaos3* tumors for NF1 and active RAS levels. The mammary tumors without detectable NF1 have homozygous deletions of *Nf1* (Table S4), whereas the bone tumor and mammary tumor 22418 contain no *Nf1* deletions. The presence of NF1 protein is inversely correlated with the level of activated (GTP-bound RAS). (B) NF1 and the Ras pathway. NF1 loss leads to increased cell proliferation and transcription of antiapoptosis genes because of failure to negatively regulate Ras. Inhibitors used in this study to slow proliferation of NF1-deficient tumor cells are shown in red type. Not all downstream targets are shown. RTK, receptor tyrosine kinase. (C) Cell proliferation assays showing sensitivity of *Chaos3* tumors to rapamycin and Mek1 inhibitor PD98059. Line colors: red, HeLa; brown, MCF-7 and MDA-MB231; blue, PyVT; and black, *Chaos3*. BT, bone tumor; MT, mammary tumor; MTCL, mammary tumor cell line.

isochore transition zone conserved between human and mouse, separating early and late replicating chromatin (Schmegner *et al.* 2005). Furthermore, collisions between replication and transcription complexes cause instability at fragile sites in the longest human genes (Helmrich *et al.* 2011). In the case of *Chaos3* cancers, there may be a predisposition for replication fork stalling at particular genomic regions that are problematic for the destabilized *Chaos3* helicase (Chuang *et al.* 2012), coupled with selective growth advantage conferred to cells by such mutations. Another curious issue has to do with strain specificity of *Chaos3* mammary tumors, which occur on the C3H but not C57BL/6J background. One possible explanation may be related to differential DNA replication mechanics *per se*. *Chaos3* cells have reduced Mcm2-7 mRNA and protein levels that lead to a decreased number of backup (“dormant”) replication

origins (Kawabata *et al.* 2011a; Chuang *et al.* 2012), and these two strains differ in the density of licensed origins (Kawabata *et al.* 2011b). Backup origins are important for rescue of stalled or collapsed DNA replication forks that may otherwise lead to chromosomal aberrations (Blow *et al.* 2011). The *Nf1* region may be particularly susceptible to stalled replication forks, and thus strain differences in backup origin density could have an impact. Alternatively, the two strains may have differential chromatin structure near *Nf1* and/or other key tumor drivers in mammary epithelial cells, leading to an increased likelihood of CNAs in those regions. Finally, there may be genetic differences between the strains that confer biological resistance or susceptibility of an unknown nature. These differences would be mappable by standard genetic crosses, lending insight into heritable factors in breast cancer.

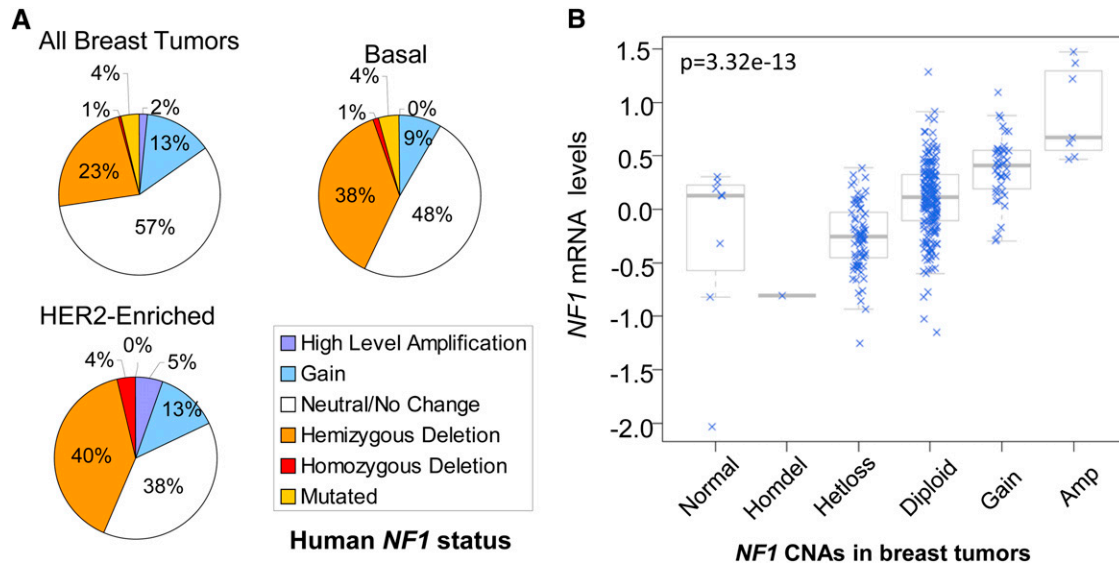


**Figure 5** Frequent *NF1* deletion in human breast cancer. (A) Percentage of *NF1* CNA and mutation in 511 human breast tumors, including 57 Her2-Enriched and 93 Basal breast tumors (publically available TCGA data). Note that 27.7% of human breast tumors have *NF1* deletion or mutation, and HER2-enriched and basal breast tumor subtypes have  $\geq 40\%$  *NF1* deletion or mutation. (B) Boxplot of *NF1* mRNA expression vs. copy number in human breast cancer. Data are from TCGA Research Network. *P*-value is for ANOVA between het-loss and diploid groups, indicating expression levels significantly correlate with genomic deletion status.

The C3H-*Chaos3* mouse has important features that make it a highly relevant breast cancer model. First, because it is not genetically engineered to lack a tumor suppressor or express an oncogene, the cancers are driven by spontaneous events. Presumably, these events are mutations arising as a secondary consequence of the *Mcm4*<sup>*Chaos3*</sup> genomic instability allele. Second, tumor differentiation score analyses of mRNA levels indicated that *Chaos3* mammary tumors more closely resemble human luminal precursors than all other characterized mouse models. Finally, the secondary mutations arising in this model are primarily interstitial CNAs that are limited in number, relatively small in size, and often have nested breakpoints that refine the “critical regions” containing potential cancer driver genes. Together, the mouse and TCGA human data indicate that *NF1* loss in conjunction with other CNAs is important for initiation and maintenance of mammary tumorigenesis in *Chaos3* mice and a substantial subset of human patients. Among the other CNAs, *Ube4b* and *Kif1b* were frequently deleted in *Chaos3* mammary tumors specifically, and human breast tumors also show frequent deletion (26%; Table 3, Table S2, and Figure S3). Genes in these and other recurrently altered regions are candidates for future studies of potential susceptibility genes underlying spontaneous or heritable forms of breast cancer.

Identification of *NF1* as a potential tumor driver in a subset of breast cancers can provide guidance for patient treatment. First, suppression of the RAS pathway would be an appropriate target. However, loss or decrease of NF1 may trigger more than RAS pathway activation, as NF1 has been shown to bind to focal adhesion kinase (FAK) and has multiple isoforms of unknown functions (Kweh *et al.* 2009). Second, there is reason to believe that tamoxifen, the estrogen

receptor (ER) inhibitor that is standard treatment for ER<sup>+</sup> breast cancers, may not be appropriate for women whose cancers involve *NF1* mutations. *NF1* depletion was reported to confer resistance of human breast cancer (MCF7) cells to tamoxifen, and tamoxifen-treated patients whose tumors had lower *NF1* expression levels had poorer clinical outcomes (Mendes-Pereira *et al.* 2012).

Based on cancer incidence estimates (Jemal *et al.* 2011; Siegel *et al.* 2012) and the frequency of *NF1* deletions (Figure 5A), ~63,450 patients in the United States and 383,230 worldwide will develop breast cancer with an *NF1* deficiency annually. Our results demonstrate a consistent pattern of spontaneous CNAs associated with mouse and human mammary tumor carcinogenesis, particularly the importance of *Nf1* deletion and provide a model for validation of these genes and drugs that target them.

## Acknowledgments

We thank R. Weiss for providing the MMTV-*Neu* tumor samples and the MDA-MB231 cell line, R. Davisson for providing the MCF-7 and HeLa cell lines, A. Nikitin for continuous advice, the Cornell Genomics Core Facility for processing our genomic samples, and the Cornell Computational Biology Service Unit for consultation on data analysis. This study was supported by National Institutes of Health training grants IT32HDO57854 and 5T32GM007617 that supported M.D.W., Empire State Stem Cell Fund contract nos. C026442 and C024174 to J.C.S., and C.M.P. and A.D.P. were supported by National Cancer Institute Breast SPORE program (P50-CA58223-09A1), U24-CA143848, and by the Breast Cancer Research Foundation.

## Literature Cited

- Arima, Y., H. Hayashi, K. Kamata, T. M. Goto, M. Sasaki *et al.*, 2009 Decreased expression of neurofibromin contributes to epithelial-mesenchymal transition in neurofibromatosis type 1. *Exp. Dermatol.* 19: e136–e141.
- Bajenaru, M. L., J. Donahoe, T. Corral, K. M. Reilly, S. Brophy *et al.*, 2001 Neurofibromatosis 1 (NF1) heterozygosity results in a cell-autonomous growth advantage for astrocytes. *Glia* 33: 314–323.
- Berger, A. H., A. G. Knudson, and P. P. Pandolfi, 2011 A continuum model for tumour suppression. *Nature* 476: 163–169.
- Blow, J. J., X. Q. Ge, and D. A. Jackson, 2011 How dormant origins promote complete genome replication. *Trends Biochem. Sci.* 36: 405–414.
- Carey, L. A., C. M. Perou, C. A. Livasy, L. G. Dressler, D. Cowan *et al.*, 2006 Race, breast cancer subtypes, and survival in the Carolina Breast Cancer Study. *JAMA* 295: 2492–2502.
- Chang, S. B., P. Miron, A. Miron, and J. D. Iglehart, 2007 Rapamycin inhibits proliferation of estrogen-receptor-positive breast cancer cells. *J. Surg. Res.* 138: 37–44.
- Chuang, C. H., M. D. Wallace, C. Abratte, T. Southard, and J. C. Schimenti, 2010 Incremental genetic perturbations to MCM2–7 expression and subcellular distribution reveal exquisite sensitivity of mice to DNA replication stress. *PLoS Genet.* 6: e1001110.
- Chuang, C. H., D. Yang, G. Bai, A. Freeland, S. C. Pruitt *et al.*, 2012 Post-transcriptional homeostasis and regulation of MCM2–7 in mammalian cells. *Nucleic Acids Res.* 40: 4914–4924.
- Curtis, C., S. P. Shah, S. F. Chin, G. Turashvili, O. M. Rueda *et al.*, 2012 The genomic and transcriptomic architecture of 2,000 breast tumours reveals novel subgroups. *Nature* 486: 346–352.
- DePristo, M. A., E. Banks, R. Poplin, K. V. Garimella, J. R. Maguire *et al.*, 2011 A framework for variation discovery and genotyping using next-generation DNA sequencing data. *Nat. Genet.* 43: 491–498.
- Ding, L., G. Getz, D. A. Wheeler, E. R. Mardis, M. D. McLellan *et al.*, 2008 Somatic mutations affect key pathways in lung adenocarcinoma. *Nature* 455: 1069–1075.
- Goettel, J. A., D. Liang, V. C. Hilliard, K. L. Edelblum, M. R. Broadus *et al.*, 2011 KSR1 is a functional protein kinase capable of serine autophosphorylation and direct phosphorylation of MEK1. *Exp. Cell Res.* 317: 452–463.
- Greenman, C., P. Stephens, R. Smith, G. L. Dalgliesh, C. Hunter *et al.*, 2007 Patterns of somatic mutation in human cancer genomes. *Nature* 446: 153–158.
- Guran, S., and M. Safali, 2005 A case of neurofibromatosis and breast cancer: loss of heterozygosity of NF1 in breast cancer. *Cancer Genet. Cytogenet.* 156: 86–88.
- Gutmann, D. H., A. Loehr, Y. Zhang, J. Kim, M. Henkemeyer *et al.*, 1999 Haploinsufficiency for the neurofibromatosis 1 (NF1) tumor suppressor results in increased astrocyte proliferation. *Oncogene* 18: 4450–4459.
- Gutmann, D. H., Y. L. Wu, N. M. Hedrick, Y. Zhu, A. Guha *et al.*, 2001 Heterozygosity for the neurofibromatosis 1 (NF1) tumor suppressor results in abnormalities in cell attachment, spreading and motility in astrocytes. *Hum. Mol. Genet.* 10: 3009–3016.
- Hanahan, D., and R. A. Weinberg, 2011 Hallmarks of cancer: the next generation. *Cell* 144: 646–674.
- Helmrich, A., M. Ballarino, and L. Tora, 2011 Collisions between replication and transcription complexes cause common fragile site instability at the longest human genes. *Mol. Cell* 44: 966–977.
- Herschkowitz, J. I., K. Simin, V. J. Weigman, I. Mikaelian, J. Usary *et al.*, 2007 Identification of conserved gene expression features between murine mammary carcinoma models and human breast tumors. *Genome Biol.* 8: R76.
- Herschkowitz, J. I., W. Zhao, M. Zhang, J. Usary, G. Murrow *et al.*, 2012 Comparative oncogenomics identifies breast tumors enriched in functional tumor-initiating cells. *Proc. Natl. Acad. Sci. USA* 109: 2778–2783.
- Hube, F., M. Mutawe, E. Leygue, and Y. Myal, 2004 Human small breast epithelial mucin: the promise of a new breast tumor biomarker. *DNA Cell Biol.* 23: 842–849.
- Jemal, A., F. Bray, M. M. Center, J. Ferlay, E. Ward *et al.*, 2011 Global cancer statistics. *CA Cancer J. Clin.* 61: 69–90.
- Kan, Z., B. S. Jaiswal, J. Stinson, V. Janakiraman, D. Bhatt *et al.*, 2010 Diverse somatic mutation patterns and pathway alterations in human cancers. *Nature* 466: 869–873.
- Kawabata, T., S. W. Luebben, S. Yamaguchi, I. Ilves, I. Matise *et al.*, 2011a Stalled fork rescue via dormant replication origins in unchallenged S phase promotes proper chromosome segregation and tumor suppression. *Mol. Cell* 41: 543–553.
- Kawabata, T., S. Yamaguchi, T. Buske, S. W. Luebben, M. Wallace *et al.*, 2011b A reduction of licensed origins reveals strain-specific replication dynamics in mice. *Mamm. Genome* 22: 506–517.
- Keane, T. M., L. Goodstadt, P. Danecek, M. A. White, K. Wong *et al.*, 2011 Mouse genomic variation and its effect on phenotypes and gene regulation. *Nature* 477: 289–294.
- Klijn, C., H. Holstege, J. de Ridder, X. Liu, M. Reinders *et al.*, 2008 Identification of cancer genes using a statistical framework for multiexperiment analysis of nondiscretized array CGH data. *Nucleic Acids Res.* 36: e13.
- Kweh, F., M. Zheng, E. Kurenova, M. Wallace, V. Golubovskaya *et al.*, 2009 Neurofibromin physically interacts with the N-terminal domain of focal adhesion kinase. *Mol. Carcinog.* 48: 1005–1017.
- Lee, J., J. Wang, M. Torbenson, Y. Lu, Q. Z. Liu *et al.*, 2010 Loss of SDHB and NF1 genes in a malignant phyllodes tumor of the breast as detected by oligo-array comparative genomic hybridization. *Cancer Genet. Cytogenet.* 196: 179–183.
- Leong, D. T., J. Lim, X. Goh, J. Pratap, B. P. Pereira *et al.*, 2010 Cancer-related ectopic expression of the bone-related transcription factor RUNX2 in non-osseous metastatic tumor cells is linked to cell proliferation and motility. *Breast Cancer Res.* 12: R89.
- Li, X. C., J. C. Schimenti, and B. K. Tye, 2009 Aneuploidy and improved growth are coincident but not causal in a yeast cancer model. *PLoS Biol.* 7: e1000161.
- Lichtenstein, P., N. V. Holm, P. K. Verkasalo, A. Iliadou, J. Kaprio *et al.*, 2000 Environmental and heritable factors in the causation of cancer—analyses of cohorts of twins from Sweden, Denmark, and Finland. *N. Engl. J. Med.* 343: 78–85.
- Lieberman, H. B., J. D. Bernstock, C. G. Broustas, K. M. Hopkins, C. Leloup *et al.*, 2011 The role of RAD9 in tumorigenesis. *Mol. cell Biol.* 3: 39–43.
- Lozano, J., R. Xing, Z. Cai, H. L. Jensen, C. Trempus *et al.*, 2003 Deficiency of kinase suppressor of Ras1 prevents oncogenic ras signaling in mice. *Cancer Res.* 63: 4232–4238.
- Mendes-Pereira, A. M., D. Sims, T. Dexter, K. Fenwick, I. Assiotis *et al.*, 2012 Genome-wide functional screen identifies a compendium of genes affecting sensitivity to tamoxifen. *Proc. Natl. Acad. Sci. USA* 109: 2730–2735.
- Munirajan, A. K., K. Ando, A. Mukai, M. Takahashi, Y. Suenaga *et al.*, 2008 KIF1Bbeta functions as a haploinsufficient tumor suppressor gene mapped to chromosome 1p36.2 by inducing apoptotic cell death. *J. Biol. Chem.* 283: 24426–24434.
- Parkin, B., P. Ouillette, Y. Wang, Y. Liu, W. Wright *et al.*, 2010 NF1 inactivation in adult acute myelogenous leukemia. *Clin. Cancer Res.* 16: 4135–4147.
- Perou, C. M., T. Sorlie, M. B. Eisen, M. van de Rijn, S. S. Jeffrey *et al.*, 2000 Molecular portraits of human breast tumours. *Nature* 406: 747–752.
- Prat, A., J. S. Parker, O. Karginova, C. Fan, C. Livasy *et al.*, 2010 Phenotypic and molecular characterization of the claudin-low intrinsic subtype of breast cancer. *Breast Cancer Res.* 12: R68.

- Pylayeva-Gupta, Y., E. Grabocka, and D. Bar-Sagi, 2011 RAS oncogenes: weaving a tumorigenic web. *Nat. Rev. Cancer* 11: 761–774.
- Robinson, J. T., H. Thorvaldsdottir, W. Winckler, M. Guttman, E. S. Lander *et al.*, 2011 Integrative genomics viewer. *Nat. Biotechnol.* 29: 24–26.
- Salemis, N. S., G. Nakos, D. Sambaziotis, and S. Gourgiotis, 2010 Breast cancer associated with type 1 neurofibromatosis. *Breast Cancer* 17: 306–309.
- Schmegner, C., A. Berger, W. Vogel, H. Hameister, and G. Assum, 2005 An isochore transition zone in the NF1 gene region is a conserved landmark of chromosome structure and function. *Genomics* 86: 439–445.
- Sharif, S., A. Moran, S. M. Huson, R. Iddenden, A. Shenton *et al.*, 2007 Women with neurofibromatosis 1 are at a moderately increased risk of developing breast cancer and should be considered for early screening. *J. Med. Genet.* 44: 481–484.
- Sherry, S. T., M. H. Ward, M. Kholodov, J. Baker, L. Phan *et al.*, 2001 dbSNP: the NCBI database of genetic variation. *Nucleic Acids Res.* 29: 308–311.
- Shima, N., A. Alcaraz, I. Liachko, T. R. Buske, C. A. Andrews *et al.*, 2007 A viable allele of Mcm4 causes chromosome instability and mammary adenocarcinomas in mice. *Nat. Genet.* 39: 93–98.
- Siegel, R., D. Naishadham, and A. Jemal, 2012 Cancer statistics, 2012. *CA Cancer J. Clin.* 62: 10–29.
- Stephens, P. J., P. S. Tarpey, H. Davies, P. Van Loo, C. Greenman *et al.*, 2012 The landscape of cancer genes and mutational processes in breast cancer. *Nature* 486: 400–404.
- The Cancer Genome Atlas Research Network, 2008 Comprehensive genomic characterization defines human glioblastoma genes and core pathways. *Nature* 455: 1061–1068.
- The Cancer Genome Atlas Research Network, 2011 Integrated genomic analyses of ovarian carcinoma. *Nature* 474: 609–615.
- Wu, H., S. L. Pomeroy, M. Ferreira, N. Teider, J. Mariani *et al.*, 2011 UBE4B promotes Hdm2-mediated degradation of the tumor suppressor p53. *Nat. Med.* 17: 347–355.

*Communicating editor: D. W. Threadgill*

# GENETICS

Supporting Information

<http://www.genetics.org/lookup/suppl/doi:10.1534/genetics.112.142802/-/DC1>

## **Comparative Oncogenomics Implicates the Neurofibromin 1 Gene (*NF1*) as a Breast Cancer Driver**

Marsha D. Wallace, Adam D. Pfefferle, Lishuang Shen, Adrian J. McNairn, Ethan G. Cerami,  
Barbara L. Fallon, Vera D. Rinaldi, Teresa L. Southard, Charles M. Perou, and John C. Schimenti

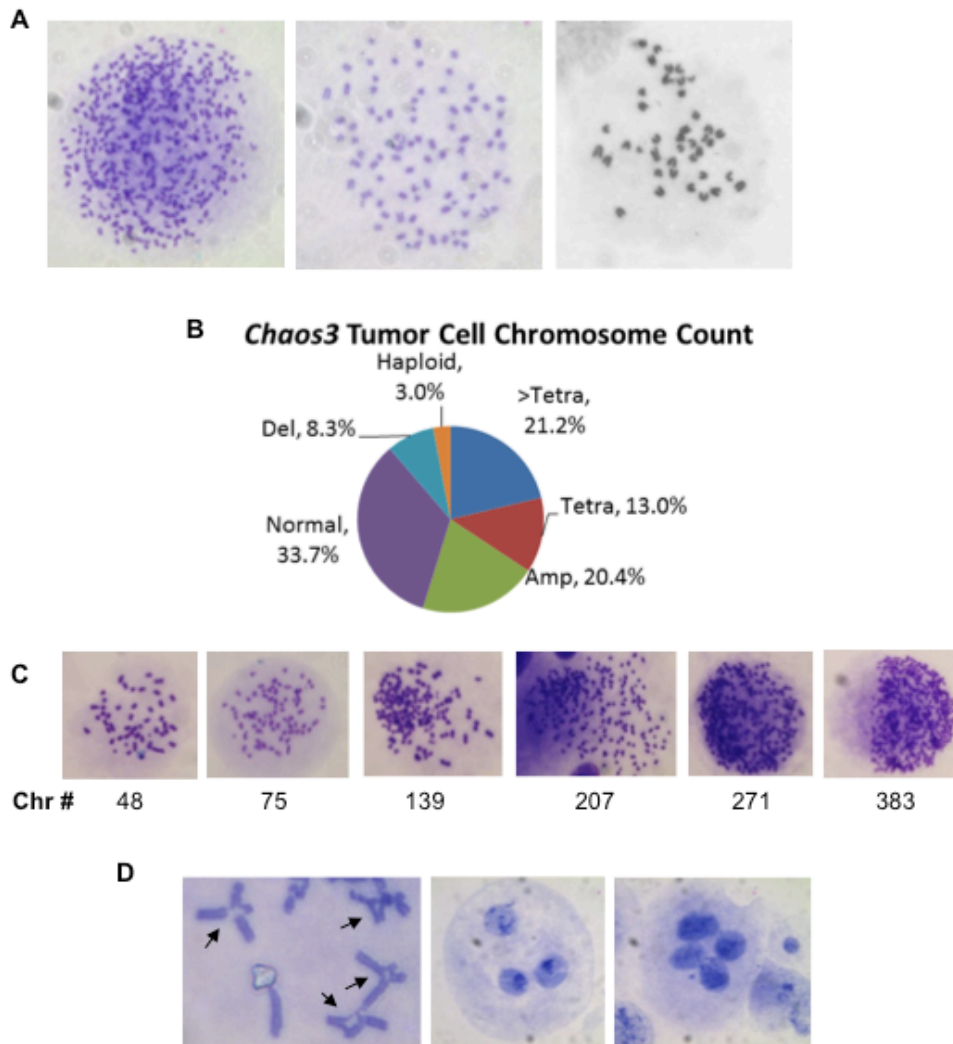


**Figure S1** *Chaos3* tumors demonstrate high levels of GIN and aneuploidy. (A) Metaphase spreads from cells of 3 *Chaos3* mammary tumors. Note aneuploidy in left and middle spreads compared to the normal 40 chromosomes (left to right: 414, 83, 40). (B) Examination of 16 *Chaos3* tumors reveal a normal chromosome count in an average of only 1/3 of the cells (>Tetra= Beyond Tetraploidy; Tetra=Tetraploid; Amp=Amplification; Del=Deletion). (C) Metaphase spreads from one *Chaos3* mammary tumor (16864a). Chromosome count is indicated beneath the images. Note the extreme variation of aneuploidy found within a single tumor. (D) Additional abnormal features displayed by tumor cells, including: cruciform structures (left) and abnormal multi-nucleated cells (middle and right).

**Mouse CNA Chr 11 78-79.6 Mb**

**Human Chr 17 22.6-26.9 Mb**

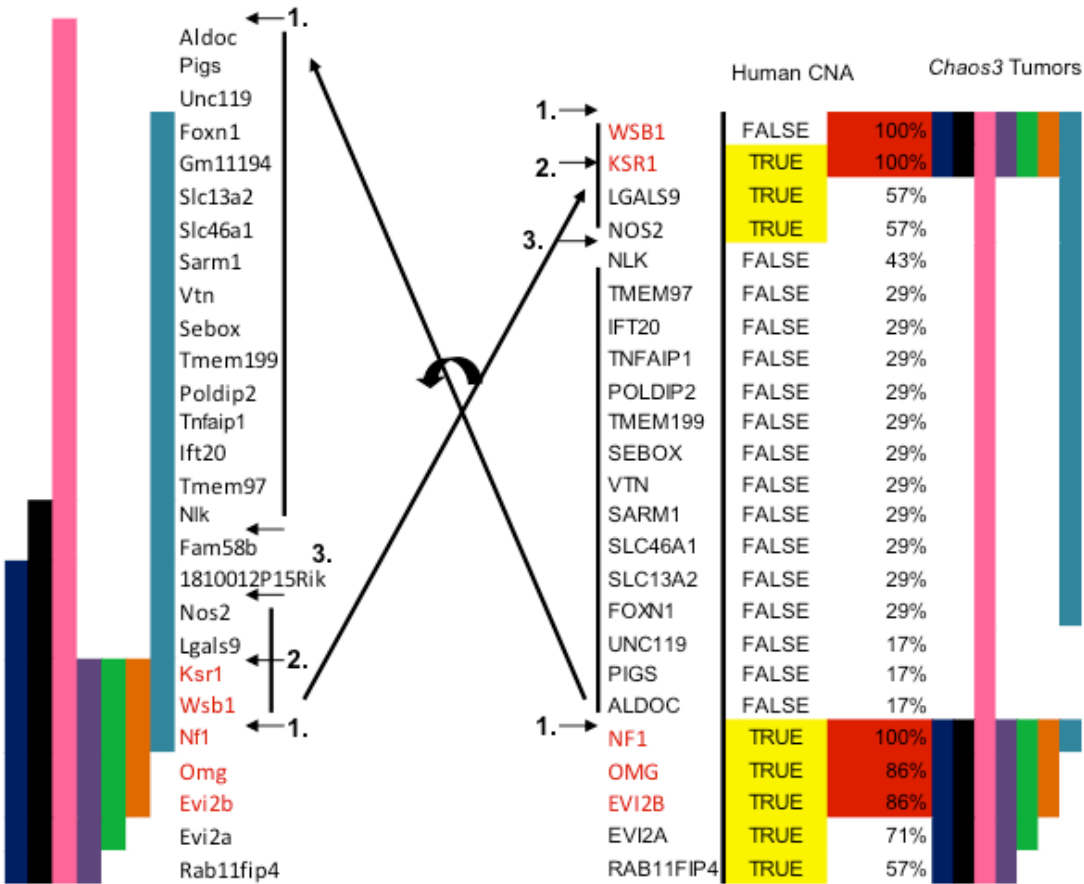


**Figure S2** Genomic sequence around *Nf1* is prone to CNA and contains a genomic rearrangement. Colored vertical bars represent the deleted region in 7 *Chaos3* mammary tumors as detected by aCGH, and the percentages reflect how many of these tumors contain CNA for a given mouse gene. Gene names in red denote the *Chaos3* critical region. Mouse and human genomic orientations of the *Nf1* region are depicted. TRUE/FALSE indicates TCGA Level 4 (limited dataset) analysis of a subset of invasive breast carcinomas for segmental CNAs; it is possible that the intervals between *NOS2* and *NF1* are actually part of more inclusive deletion events. Numbers in bold with small arrows indicate positions of interest: **1.** Proximal to *Nf1*, a breakpoint of chromosomal inversion between human and mouse occurred between and including *Wsb1* to *Aldoc*. This is a site of both human and mouse tumor CNA, and the human CNA begins with *NF1*. **2.** The mouse critical CNA begins at *Ksr1*, which has flipped orientation in humans and starts/forms a second smaller CNA, with the caveats mentioned above. **3.** The mouse genome has an insertion between *Nlk* and *Nos2*, where human statistically-declared CNAs end.

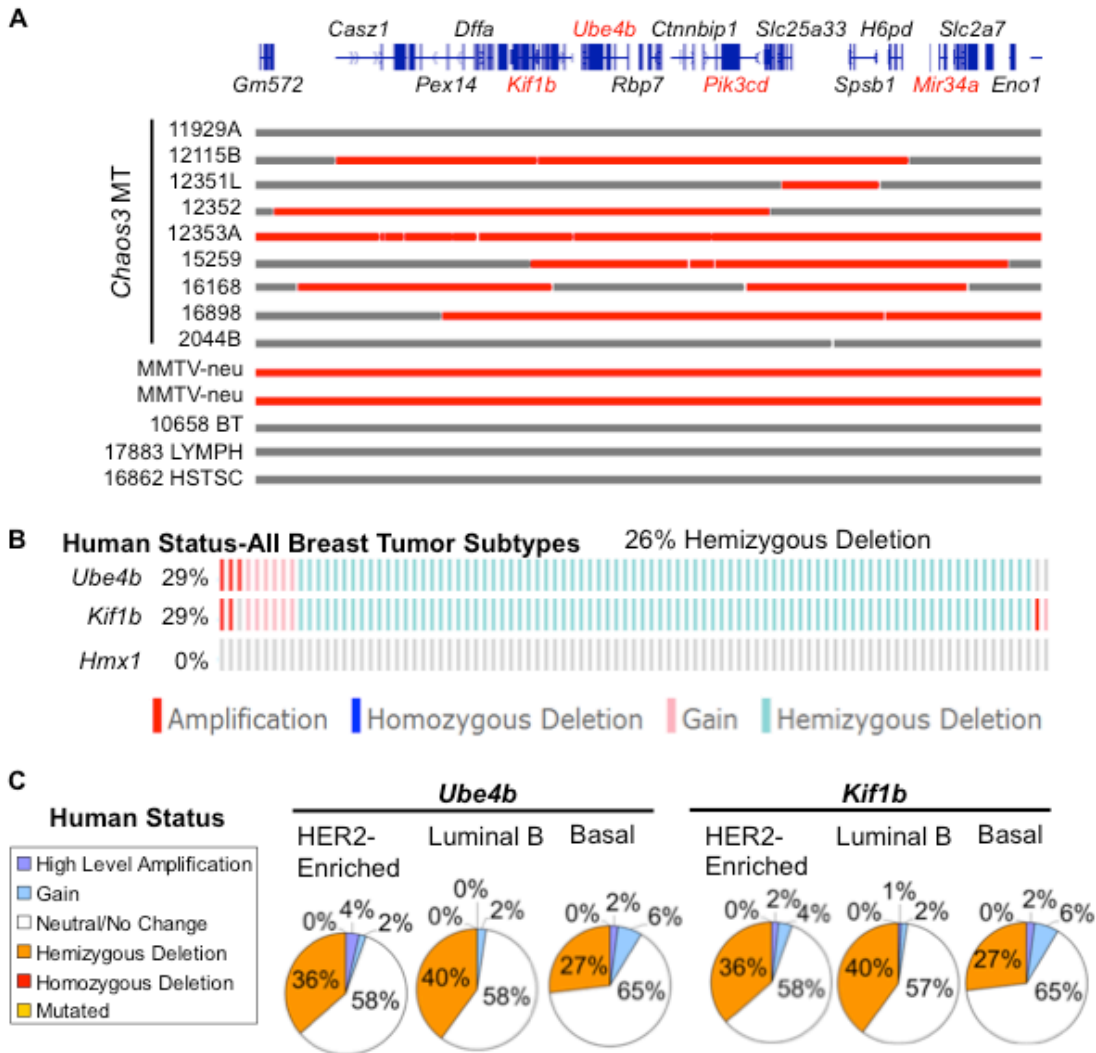


**Figure S3** *Ube4b* and *Kif1b*, deleted in over half of *Chaos3* mammary tumors, show frequent deletion in human breast tumors. (A) Recurrent Chr 4 deletions specific to mammary tumors (MT). Horizontal bars represent tumors examined by aCGH. Red portions of bars indicate deleted regions in *Chaos3* and MMTV-neu MTs. Cancer-related genes are in red. Note that *Chaos3* non-MTs do not demonstrate this deletion. BT=bone tumor; LYMPH = Lymphoma; HSTSC=histiocytic sarcoma. (B) “Oncoprints” of *Ube4b* and *Kif1b* alterations in 320 human breast tumors (TCGA data) generated by the cBio portal (see Methods). Rows contain bars representing individual tumors, and samples are aligned for visualization of alterations within the same tumor across multiple genes. *Hmx1* does not have a known role in cancer. (C) Percentage of *Ube4b* and *Kif1b* CNAs in 55 Her2-Enriched, 125 Luminal B, and 93 Basal human breast tumors (TCGA). Note that ~40% of HER2-Enriched and Luminal B tumors have hemizygous deletion of *Ube4b* and *Kif1b*, as do 27% of Basal-type breast tumors.

Files S1-S4  
Supporting Data

Available for download at <http://www.genetics.org/lookup/suppl/doi:10.1534/genetics.112.142802/-/DC1>.

**Table S1 Validated Gene Mutations in *Chaos3* Mammary Tumors**

Sample	Name	Mutation	Effect	Description	Function
15259	Myo1g	G/A	Splice Site	Myosin-Ig	Precursor of minor histocompatibility antigen HA-2
2042	Acsf6	G/T	E>D	Long-chain-fatty-acid--CoA ligase 6	Catalyze formation of acyl-CoA from fatty acids, ATP, and CoA.
2042	Tdrd6	T/C	H>R	Tudor domain-containing protein 6	Required for spermiogenesis, chromatoid body architecture, and regulation of miRNA expression.
2042	Ttn	C/T	D>N	Titin (Connectin)	Cardiac and skeletal muscle protein. Disease Associations: Familial Cardiomyopathy, Tibial muscular dystrophy
2044b	Ttn	C/G	V>L	Titin (Connectin)	

Note: The mutations were validated by Sanger sequencing of PCR products.

Table S2 *Chaos3*-specific and Mammary Tumor-specific Recurrent Deletions Overlapping Human Breast Cancer CNAs.

Mouse CNA	Gene	Hum Chr	Human CNA	<i>Chaos3</i> CNA	Tumors									
					A	B	C	D	E	F	G	H	I	
Mmu Chr 4 148.4-149.5 Mb	SLC2A7	1	FALSE	33%		x				x				
	SLC2A5	1	FALSE	50%		x				x	x			
	GPR157	1	FALSE	50%		x				x	x			
	MIR34A	1	FALSE	50%		x				x	x			
	H6PD	1	FALSE	57%		x				x	x	x		
	SPSB1	1	FALSE	86%		x	x			x	x	x	x	
	SLC25A33	1	FALSE	86%		x	x			x	x	x	x	
	TMEM201	1	FALSE	86%		x	x			x	x	x	x	
	PIK3CD	1	FALSE	86%		x			x	x	x	x	x	
	CLSTN1	1	FALSE	71%		x			x	x		x	x	
	CTNNBIP1	1	FALSE	71%		x			x	x		x	x	
	LZIC	1	FALSE	71%		x			x	x		x	x	
	NMNAT1	1	FALSE	71%		x			x	x		x	x	
	RBP7	1	FALSE	71%		x			x	x		x	x	
	UBE4B	1	TRUE	71%		x			x	x		x	x	
	KIF1B	1	TRUE	71%		x			x	x		x	x	
	PGD	1	TRUE	33%			x		x					x
	APITD1	1	TRUE	33%			x		x					x
	CORT	1	TRUE	33%			x		x					x
	DFFA	1	TRUE	33%			x		x					x
	PEX14	1	TRUE	33%			x		x					x
	CASZ1	1	TRUE	33%			x		x					
	TARDBP	1	FALSE	17%			x							
MASP2	1	FALSE	17%			x								
SRM	1	FALSE	17%			x								
Mmu Chr 5 122-125 Mb	CLIP1	12	FALSE	43%	x	x							x	
	ZCCHC8	12	FALSE	43%	x	x							x	
	RSRC2	12	FALSE	43%	x	x							x	
	KNTC1	12	FALSE	71%	x	x		x				x		x
	GPR81	12	FALSE	71%	x	x		x				x		x
	DENR	12	FALSE	71%	x	x		x				x		x
	CCDC62	12	FALSE	71%	x	x		x				x		x
	HIP1R	12	FALSE	71%	x	x		x				x		x
	VPS37B	12	FALSE	86%	x	x	x	x				x		x
	ABCB9	12	FALSE	86%	x	x	x	x				x		x
	OGFOD2	12	FALSE	86%	x	x	x	x				x		x
	ARL6IP4	12	FALSE	86%	x	x	x	x				x		x
	PITPNM2	12	FALSE	86%	x	x	x	x				x		x
	MPHOSPH9	12	FALSE	86%	x	x	x	x				x		x
	CDK2AP1	12	FALSE	86%	x	x	x	x				x		x
SBNO1	12	FALSE	86%	x	x	x	x				x		x	

	SETD8	12	FALSE	86%	x	x	x	x		x	x		
	RILPL2	12	FALSE	86%	x	x	x	x		x	x		
	SNRNP35	12	FALSE	100%	x	x	x	x		x	x		
	RILPL1	12	FALSE	100%	x	x	x	x		x	x		
	TMED2	12	FALSE	100%	x	x	x	x		x	x		
	DDX55	12	FALSE	100%	x	x	x	x		x	x		
	EIF2B1	12	FALSE	100%	x	x	x	x		x	x		
	GTF2H3	12	FALSE	100%	x	x	x	x		x	x		
	TCTN2	12	FALSE	100%	x	x	x	x		x	x		
	ATP6V0A2	12	FALSE	43%					x		x		
	CCDC92	12	FALSE	29%						x	x		
	Zfp664	12	FALSE	14%						x			
	Fam101a	12	TRUE	14%						x			
	Ncor2	12	TRUE	14%						x			
	Scarb1	12	FALSE	14%						x			
<b>Mmu Chr 11</b> 78-79.6 Mb	WSB1	17	FALSE	100%	x	x	x	*	x	*	x	x	x*
	KSR1	17	TRUE	100%	x	x	x	*	x	*	x	x	x*
	LGALS9	17	TRUE	57%		x		x*		x*		x	x*
	NOS2	17	TRUE	57%		x		x*		*		x	
	NLK	17	FALSE	43%		x				x*		x	
	TMEM97	17	FALSE	29%		x				*		x	
	IFT20	17	FALSE	29%		x				*		x	
	TNFAIP1	17	FALSE	29%		x				x*		x	
	POLDIP2	17	FALSE	29%		x						x	
	TMEM199	17	FALSE	29%		x						x	
	SEBOX	17	FALSE	29%		x						x	
	VTN	17	FALSE	29%		x						x	
	SARM1	17	FALSE	29%		x						x	
	SLC46A1	17	FALSE	29%		x						x	
	SLC13A2	17	FALSE	29%		x						x	
	FOXN1	17	FALSE	29%		x						x	
	UNC119	17	FALSE	17%		x							
	PIGS	17	FALSE	17%		x							
	ALDOC	17	FALSE	17%		x							
		NF1	17	TRUE	100%	x	x	x	x*	x	x*	x	x
	OMG	17	TRUE	86%	x	x	x	x*	x		x		x
	EVI2B	17	TRUE	86%	x	x	x	*	x		x		x
	EVI2A	17	TRUE	71%	x	x	x	*	x		x		
	RAB11FIP4	17	TRUE	57%	x	x	x	x*	x				

**Legend.** x= deleted as determined by aCGH analysis. Some qPCR genotyping from the Chr 11 interval was added, and deleted probes are indicated as x\*. Presumed deleted probes are indicated by "\*". Tumor Codes: A: 2044B; B: 12353A; C: 12351L; D: 12352; E: 15259; F: 16168; G: 12115B; H: 16898; I: 11929A. Mmu = *Mus musculus*. Some of the deletions extend further than indicated. The True (deleted) and False (not deleted) calls for human gene deletions are from TCGA level 4 data (see Methods) and refer to whether that locus is deleted at levels statistically above background. Human genes in red are potentially cancer-relevant if deleted. Red shaded regions are the "critical regions" of a deletion set. Note that the Mmu Chr 11 deletion cluster is organized in the human genome order, which is inverted and has an insertion. Thus, the critical region is actually contiguous. The "Chaos3 CNA" column refers to the % of Chaos3 mammary tumors analyzed by aCGH that contained deletions of that particular locus. ND=no data.

**Table S3** *Chaos3* Mammary Tumor Non-specific Recurrent Deletions Overlapping Human Breast Cancer CNAs.

Mouse Region	Human Gene	Hs		<i>Chaos3</i>								
		Chr	Human CNA	CNA	A	B	C	D	E	F	G	
<b>Mmu Chr 4</b> 132.4-133.5 Mb	AIM1L	1	FALSE	43%		x	x				x	
	LIN28	1	FALSE	71%		x	x	x			x	x
	DHDDS	1	FALSE	71%		x	x	x			x	x
	HMG2	1	FALSE	71%		x	x	x			x	x
	RPS6KA1	1	FALSE	86%		x	x	x	x	x	x	x
	ARID1A	1	FALSE	100%	x	x	x	x	x	x	x	x
	PIGV	1	FALSE	100%	x	x	x	x	x	x	x	x
	ZDHHC18	1	TRUE	86%	x	x	x		x	x	x	
	SFN	1	TRUE	86%	x	x	x		x	x	x	
	GPN2	1	TRUE	86%	x	x	x		x	x	x	
	GPATCH3	1	TRUE	86%	x	x	x		x	x	x	
	NR0B2	1	TRUE	86%	x	x	x		x	x	x	
	NUDC	1	TRUE	86%	x	x	x		x	x	x	
	TRNP1	1	TRUE	86%	x	x	x		x	x	x	
	FAM46B	1	FALSE	86%	x	x	x		x	x	x	
	SLC9A1	1	FALSE	71%	x		x		x		x	x
	WDTC1	1	FALSE	43%	x				x			x
	TMEM222	1	FALSE	43%	x				x			x
	SYTL1	1	FALSE	43%	x				x			x
	MAP3K6	1	FALSE	43%	x				x			x
	CD164L2	1	FALSE	43%	x				x			x
	GPR3	1	FALSE	43%	x				x			x
<b>Mmu Chr 10</b> 79.4-80.2 Mb	PPAP2C	19	TRUE	33%				x	x			
	MIER2	19	TRUE	33%				x	x			
	THEG	19	TRUE	33%				x	x			
	C2CD4C	19	TRUE	33%				x	x			
	SHC2	19	TRUE	33%				x	x			
	ODF3L2	19	TRUE	33%				x	x			
	MADCAM1	19	TRUE	33%				x	x			
	CDC34	19	TRUE	33%				x	x			
	GZMM	19	TRUE	33%				x	x			
	BSG	19	TRUE	33%				x	x			
	HCN2	19	TRUE	33%				x	x			
	POLRMT	19	TRUE	33%				x	x			
	FGF22	19	TRUE	33%				x	x			
	RNF126	19	TRUE	33%				x	x			
	FSTL3	19	TRUE	33%				x	x			
	PRSSL1	19	TRUE	33%				x	x			
	PALM	19	TRUE	33%				x	x			
	PTBP1	19	TRUE	33%				x	x			
	PRTN3	19	TRUE	33%				x	x			
	ELANE	19	TRUE	33%				x	x			

CFD	19	TRUE	33%		x	x	
MED16	19	TRUE	33%		x	x	
KISS1R	19	TRUE	50%		x	x	x
ARID3A	19	TRUE	50%		x	x	x
WDR18	19	TRUE	50%		x	x	x
GRIN3B	19	TRUE	50%		x	x	x
CNN2	19	TRUE	50%		x	x	x
ABCA7	19	TRUE	50%		x	x	x
HMHA1	19	TRUE	50%		x	x	x
POLR2E	19	TRUE	50%		x	x	x
GPX4	19	TRUE	50%		x	x	x
SBNO2	19	TRUE	50%		x	x	x
STK11	19	TRUE	50%		x	x	x
ATP5D	19	TRUE	50%		x	x	x
MIDN	19	TRUE	50%		x	x	x
CIRBP	19	TRUE	33%		x	x	
EFNA2	19	TRUE	33%		x	x	
MUM1	19	TRUE	33%		x	x	
NDUFS7	19	TRUE	33%		x	x	
GAMT	19	TRUE	33%		x	x	
DAZAP1	19	TRUE	33%		x	x	
RPS15	19	TRUE	33%		x	x	
APC2	19	TRUE	33%		x	x	
PCSK4	19	TRUE	33%		x	x	
REEP6	19	TRUE	33%		x	x	
ADAMTSL5	19	TRUE	33%		x	x	
MEX3D	19	TRUE	50%		x	x	x
MBD3	19	TRUE	50%		x	x	x
TCF3	19	TRUE	50%		x	x	x
ONECUT3	19	TRUE	67%	x	x	x	x
ATP8B3	19	TRUE	67%	x	x	x	x
REXO1	19	TRUE	67%	x	x	x	x
KLF16	19	TRUE	67%	x	x	x	x
SCAMP4	19	TRUE	67%	x	x	x	x
ADAT3	19	TRUE	67%	x	x	x	x
CSNK1G2	19	TRUE	67%	x	x	x	x
BTBD2	19	TRUE	67%	x	x	x	x
MKNK2	19	TRUE	67%	x	x	x	x
MOBKL2A	19	TRUE	67%	x	x	x	x
AP3D1	19	TRUE	67%	x	x	x	x
DOT1L	19	TRUE	67%	x	x	x	x
PLEKHJ1	19	TRUE	67%	x	x	x	x
SF3A2	19	TRUE	67%	x	x	x	x
AMH	19	TRUE	67%	x	x	x	x
JSRP1	19	TRUE	67%	x	x	x	x
OAZ1	19	TRUE	67%	x	x	x	x

LINGO3	19	TRUE	67%	x	x	x	x
LSM7	19	TRUE	33%		x	x	
TMPRSS9	19	FALSE	33%		x	x	
TIMM13	19	FALSE	33%		x	x	
LMNB2	19	FALSE	33%		x	x	
GADD45B	19	FALSE	17%		x		

**Legend.** x= deleted. Tumor Codes: A: 15259; B: 12353A; C: 12115B; D: 11929A; E: 16898; F: 2044B; G: 16892. Mmu = *Mus musculus*. Hs = *Homo sapiens*. Some of the deletions extend further than indicated. The True (deleted) and False (not deleted) calls for human gene deletions are from TCGA level 4 data (see Methods) and refer to whether that locus is deleted at levels statistically above background. Human genes in red are potentially cancer-relevant. Red shaded regions are the “critical regions” of a deletion set. The “Chaos3 CNA” column refers to the % of Chaos3 mammary tumors analyzed by aCGH that contained deletions of that particular locus.

Table S4 qPCR analysis of *Nf1* locus in tumors

Geno & Type	Tumor #	<i>Nf1</i> 5'	<i>Nf1</i> 3' ( <i>Omg</i> )
Chaos3 MT	15259	17.4	52.9
Chaos3 MT	12351 L	35.5	12.0
Chaos3 MT	12353A	25.5	16.7
Chaos3 MT	12352	12.7	0.7
Chaos3 MT	2044B CL	63.7	48.0
Chaos3 MT	11929A	16.7	16.3
Chaos3 MT	16168	9.2	ND
Chaos3 MT	16898	9.6	75.1
Chaos3 MT	12115B	31.2	38.7
Chaos3 MT	2042 CL	78.9	92.3
Chaos3 MT	919 CL	51.8	0.1
Chaos3 MT	21040	0.1	0.1
Chaos3 MT	21253	0.3	0.2
Chaos3 MT	20317	29.5	48.7
Chaos3 MT	19957	32.7	5.4
Chaos3 MT	19958	11.2	12.4
Chaos3 MT	19959	14.4	72.4
Chaos3 MT	20783	7.0	10.4
Chaos3 MT	20164	20.6	22.8
Chaos3 MT	20888	27.3	26.0
Chaos3 MT	20892	6.4	34.9
Chaos3 MT	20893	7.4	24.5
Chaos3 MT	20138	41.1	10.8
Chaos3 MT	21039	68.4	66.7
Chaos3 MT	21809	62.0	60.0
Chaos3 MT	20894	85.1	67.1
Chaos3 MT	20889	12.0	18.4
Chaos3 MT	21333	40.8	71.4
Chaos3 MT	20626	36.7	22.6
Chaos3 MT	20318	14.5	24.9
Chaos3 MT	20890	13.6	38.9
Chaos3 MT	20891	2.5	1.4
Chaos3 MT	21123	34.7	39.0
Chaos3 MT	19660	44.8	48.3
Chaos3 MT	20459	53.7	69.8
Chaos3 MT	21597	28.6	5.3
Chaos3 MT	22182	62.6	78.2
Chaos3 MT	21416	63.8	56.8
Chaos3 MT	22236	31.6	8.0
Chaos3 MT	22418	24.9	24.2
Chaos3 MT	22180	23.9	49.0
Chaos3 MT	22235	8.1	8.2
Chaos3 MT	22166	21.7	21.0
Chaos3 MT	22168	8.0	7.6
Chaos3 MT	22238	3.4	3.4

Chaos3 MT	21417	3.3	14.8
Chaos3 MT	21419	19.2	50.6
Chaos3 MT	21255	7.0	6.1
Chaos3 MT	21124	8.5	29.1
Chaos3 MT	21810	26.3	27.0
Chaos3 MT	21811	47.3	51.7
Chaos3 MT	21254	9.5	7.9
Chaos3 MT	21041	24.4	21.2
Chaos3 MT	22420	40.5	17.1
Chaos3 MT	22476	75.5	70.7
Chaos3 MT	22414	3.3	17.1
Chaos3 MT	22416	3.5	14.6
Chaos3 MT	22417	7.1	19.4
Chaos3 MT	23116	11.2	10.8
Chaos3 MT	22418	115.0	110.3
Chaos3 non-MT	19160	198.2	207.5
Chaos3 non-MT	10658	87.1	ND
Chaos3 non-MT	16862	98.5	101.2
Chaos3 non-MT	17883	97.0	88.0
PyVT		96.3	105.1
MMTV-neu1		108.6	93.2
MMTV-neu2		103.8	104.4
Chaos3 +/- MT		107.3	109.4

**Legend.** qPCR values are presented as the percentage vs C3H DNA. *Nf1* probes were at the 5' and 3' ends of the gene. The 3' probe actually corresponds to the *Omg* gene that lies within an *Nf1* intron near the 3' end. Note that copy number differences between the *Nf1* 5' and 3' are observed in some tumors, indicating a breakpoint within *Nf1*. Deletion calls were made as follows: Heterozygous = 15-80%; Homozygous = <15%. If either *Nf1* or *Omg* were <15%, the tumor sample was called as homozygous deleted because full *Nf1* transcripts cannot be made. MT = mammary tumor.